Simulation of Water Sources and Precipitation Recycling for the MacKenzie, Mississippi, and Amazon River Basins

MICHAEL G. BOSILOVICH AND JIUN-DAR CHERN

Global Modeling and Assimilation Office, NASA Goddard Space Flight Center, Greenbelt, Maryland

(Manuscript received 10 March 2005, in final form 17 August 2005)

ABSTRACT

An atmospheric general circulation model simulation for 1948–97 of the water budgets for the MacKenzie, Mississippi, and Amazon River basins is presented. In addition to the water budget, passive tracers are included to identify the geographic sources of water for the basins, and the analysis focuses on the mechanisms contributing to precipitation recycling in each basin. While each basin's precipitation recycling has a strong dependency on evaporation during the mean annual cycle, the interannual variability of the recycling shows important relationships with the atmospheric circulation. The MacKenzie River basin recycling has only a weak interannual correspondence with evaporation, where the variations in zonal moisture transport from the Pacific Ocean can affect the basin water cycle. On the other hand, the Mississippi River basin precipitation and recycling have strong interannual correlation on evaporation. The evaporation is related to the moist and shallow planetary boundary layer that provides moisture for convection at the cloud base. At global scales, high precipitation recycling is also found to be partly correlated to warm SSTs in the tropical Pacific Ocean. The Amazon River basin evaporation exhibits small interannual variations, so the interannual variations of precipitation recycling are related to atmospheric moisture transport from the tropical South Atlantic Ocean. Increasing SSTs over the 50-yr period are causing increased easterly transport across the basin. As moisture transport increases, the Amazon precipitation recycling decreases (without real-time varying vegetation changes). In addition, precipitation recycling from a bulk diagnostic method is compared to the passive tracer method used in the analysis. While the mean values of the different recycling methods are different, the interannual variations are comparable between each method. The methods also exhibit similar relationships to the terms of the basin-scale water budgets.

1. Introduction

When analyzing water cycle intensity, regional variations can be significantly different from the global background (e.g., Bosilovich et al. 2005). Precipitation over land is a function of both transport of water from the oceans and the evaporation from the land (Trenberth et al. 2003). The water holding capacity of the vegetation and soil limits land evaporation. Therefore, variations of the land evaporation can affect the surface energy budget, planetary boundary layer, and the convective potential energy of the atmospheric column (Betts 2004), and ultimately the feedback with precipitation. Persistence of soil moisture anomalies can lead to prolonged variations in the regional intensity of the water cycle (e.g., droughts or floods: Schubert et al. 2004a,b). The regional intensity of the water cycle can be quantified by calculating the local precipitation recycling (Brubaker et al. 1993; Eltahir and Bras 1996; Dirmeyer and Brubaker 1999; Bosilovich and Schubert 2001, 2002; Stohl and James 2004; Yoshimura et al. 2004). Precipitation recycling is defined as the "contribution of local evaporation to local precipitation," specifically delineating the source of mass of water in precipitation between local and remote geographic sources (Eltahir and Bras 1996). This can be used to characterize and quantify the intensity of the regional water cycle.

Two recent studies provide the impetus for the numerical experiment presented here. Brubaker et al. (2001) showed the long-term analysis of evaporative sources for the Mississippi River basin (MRB). Variations of evaporative oceanic sources can affect the recycling of precipitation. In addition, over 36 years some significant trends in sources of water for the basin were

Corresponding author address: Michael G. Bosilovich, Global Modeling and Assimilation Office, Code 610.1, NASA Goddard Space Flight Center, Greenbelt, MD 20771.
E-mail: Michael.Bosilovich@nasa.gov

© 2006 American Meteorological Society

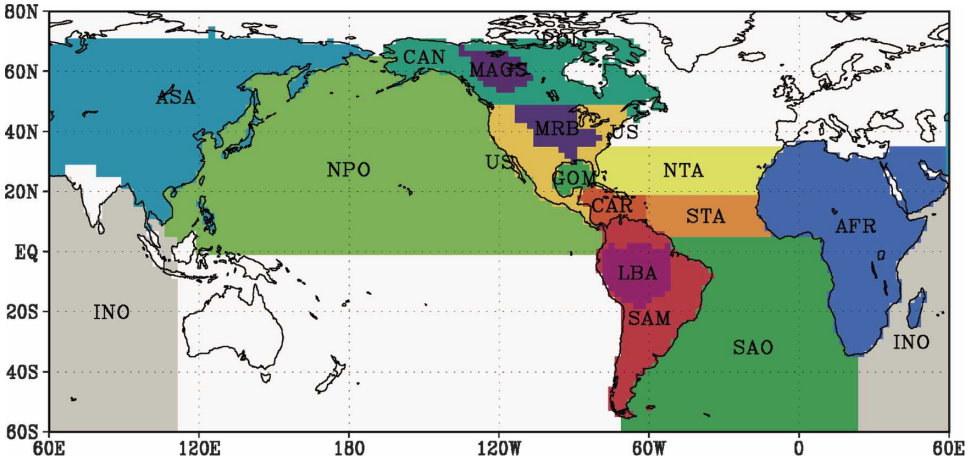

FIG. 1. Map of source regions for water vapor tracers (WVTs), where each color indicates a different evaporative source region. The regions are the MacKenzie Area GEWEX Study: MAGS, Mississippi River basin: MRB, Large-scale Biosphere Atmosphere Experiment for the Amazon: LBA, North Pacific Ocean: NPO, South Atlantic Ocean: SAO, south tropical Atlantic Ocean: STA, north tropical Atlantic Ocean: NTA, Caribbean Sea: CAR, Gulf of Mexico: GOM, Indian Ocean: INO, Africa: AFR, Asia: ASA, Canada: CAN, and South America: SAM. The land area to the east and west of MRB, including Mexico, is included in a WVT called US.

identified. Second, Bosilovich et al. (2005) evaluated climate atmospheric general circulation model (AGCM) simulations for a 50-yr duration. The AGCMs show global increasing trends of precipitation, but the trend of precipitation over land was decreasing. The regional trends of precipitation differed in sign, magnitude, and statistical significance. The regional evaluation of water cycle intensity and the influence of local and large-scale processes were not investigated.

To better understand regional water cycles, the local interactions and the atmospheric circulation variations especially regarding precipitation recycling, we have run a 50-yr AGCM simulation (with prescribed SSTs), including diagnostics for the geographical sources of water vapor and precipitation recycling. In this paper, we focus on the water sources and precipitation recycling for the Global Energy and Water Cycle Experiment (GEWEX) Continental-scale Experiments (CSEs) in the Americas (Fig. 1). The MacKenzie GEWEX Study (MAGS) represents a high-latitude basin. The MRB is a midlatitude basin with crucial agricultural production in the world economy [included in the GEWEX Americas Prediction Project (GAPP CSE)]. The Large-scale Biosphere–Atmosphere Experiment for the Amazon (LBA) is a tropical region where the local water cycle represents a substantial fraction of the globe, and where precipitation recycling has been studied for a long time. While other basins in Europe and Asia are important in their own ways, these three represent a subset of different climate regimes for comparison.

2. Model and methodology

a. Finite-volume general circulation model

The atmospheric numerical model used in this study is the finite-volume general circulation model (fvGCM) (Lin 2004). The finite-volume dynamical core uses a terrain-following Lagrangian control-volume vertical coordinate system (Lin 2004; Collins et al. 2004). The fvGCM dynamical core includes a conservative semi-Lagrangian transport algorithm. The algorithm has consistent and conservative transport of air mass and absolute vorticity (Lin and Rood 1997). This feature of the system makes the fvGCM particularly useful for water vapor and passive tracer simulations.

The physical parameterizations of the fvGCM are based on National Center for Atmospheric Research (NCAR) Community Climate Model version 3.0 (CCM3) physics. The NCAR CCM3 parameterizations are a collection of physical processes with a long history of development and documentation (Kiehl et al. 1998). The moist physics package includes the Zhang and McFarlane (1995) deep convective scheme, which handles updrafts and downdrafts and operates in conjunction with the Hack (1994) mid and shallow convection scheme. Bosilovich et al. (2003) validate regional aspects of the simulated hydrological cycle. This version of the fvGCM uses the Common Land Model [version 2, described by Dai et al. (2003) and Oleson et al. (2004)]. Bonan et al. (2002) and Zeng et al. (2002) evaluate the implementation of the CLM in the NCAR community GCM.

b. Precipitation recycling

The model also includes water vapor tracers (WVTs) to quantify the geographical source of water for global precipitation (Bosilovich and Schubert 2002; Bosilovich 2002; Bosilovich et al. 2003). In this configuration, the source of water for a tracer is the evaporation from a predefined region (e.g., Fig. 1). This humidity is then predicted as a passive tracer (separate and distinct from the model's specific humidity prognostic variable) including tracer transport and precipitation and turbulent tendencies, using

$$\frac{\partial q_T}{\partial t} = -\nabla_3 \cdot (q_T \mathbf{V}) + \frac{\partial q_T}{\partial t}_{\text{turb}} + \frac{\partial q_T}{\partial t}_{\text{prec}}, \tag{1}$$

where q_T is the three-dimensional water vapor tracer, $\mathbf{V}$ is the three-dimensional wind, "turb" denotes the turbulent tendency not including surface evaporation (vertically integrates to zero), and "prec" denotes the sum of all tracer precipitation tendencies (including condensation, rain evaporation, and convective vertical movement; this term vertically integrates to the tracer precipitation, $-P_T$). The tracer precipitation tendencies are computed proportional to the total precipitation tendency, where the proportionality is based on the ratio of tracer water to total water (Bosilovich and Schubert 2002).

The WVT methodology requires a modest investment in developing the code and also computing additional atmospheric prognostic variables. Precipitation recycling (but not specific external sources) can also be determined by simpler bulk diagnostic methods (e.g., Brubaker et al. 1993). The bulk diagnostic methods use monthly moisture transport and surface evaporation to solve a regional water budget. The inflowing atmospheric moisture can be computed from the line integration of monthly moisture transport as

$$Q_{\text{in}} = \frac{-1}{A\rho_w g}\oint \Delta p \langle q\mathbf{V}\rangle \cdot \mathbf{n}\, dl_{\text{in}}\,, \tag{2}$$

where A is the area of the basin (in m^2), g is the acceleration of gravitation (9.81 m s^{-2}), ρ_w is the density of water (1000 kg m^{-3}), Δp is the pressure thickness of the entire column of the model's atmosphere (in pascals), $\langle q\mathbf{V}\rangle$ indicates the vertically integrated moisture transport vector (integrated from the model's vertical coordinate, in units of m s^{-1} kg of water per kilogram of air). Here $\mathbf{n}$ is the outward unit normal vector (dimensionless) and dl_{in} indicates that the line integration only considers segments of the gridded data where water is flowing into the basin (units of m). With a unit conversion, the inflowing moisture transport (Q_{in}) is calculated in units of mm day^{-1}. Following Brubaker et al. (1993), specifically their Eqs. (7) and (12), we can compute the recycling ratio for the basin from the inflowing moisture transport and basin averaged evaporation (E in mm day^{-1}),

$$\rho_B = \frac{P_{\text{local}}}{P_{\text{total}}} = \frac{E}{2Q_{\text{in}} + E}\,, \tag{3}$$

where the bulk diagnostic recycling ratio (ρ_B) is defined as the ratio of precipitation from local evaporation to the total precipitation that occurs. The bulk diagnostic recycling ratio can be compared to the value determined from the WVT method.

c. Experimental design

The model simulation is evaluated for 50 years, from the beginning of 1948 through the end of 1997. Hadley Centre SSTs provide the prescribed oceanic boundary conditions for the AGCM (Rayner et al. 1996, 2003). The experiment is similar to the first phase of the Climate of the Twentieth Century study (Folland et al. 2002) in that it uses prescribed SST variations, but not aerosols, carbon cycle, or other climate change input forcing (e.g., vegetations cover). The spatial resolution of the model grid is 2° latitude by 2.5° longitude. The initial conditions were derived from a longer simulation (started in 1901), and tracers were initialized at zero in September 1947. A total of 36 WVTs were defined by geographic location (Fig. 1 only shows those relevant to the regional analysis discussed here). The basin areas were defined by interpolating the mask used by Roads et al. (2002) to the model's grid. The tracers are spun up within weeks of initialization (Bosilovich and Schubert 2002).

3. Simulated seasonal cycle and interannual variability

Figure 2 compares the seasonal variations of precipitation of the model with the merged Global Precipitation Climatology Project (GPCP) product (Adler et al. 2003) for the region of this investigation. The model produces large-scale convergent and divergent patterns that can be identified by the precipitation field. Over the domain, there is an overestimate of precipitation. The most noticeable overestimates occur off the west coast of Central America in September–October (SON) and December–February (DJF). Despite this, it is interesting to note that the model seems to underestimate precipitation in the easternmost region of the intertropical convergence zone (ITCZ) during June–August (JJA). The simulated precipitation across North America in JJA seems comparable to the merged data

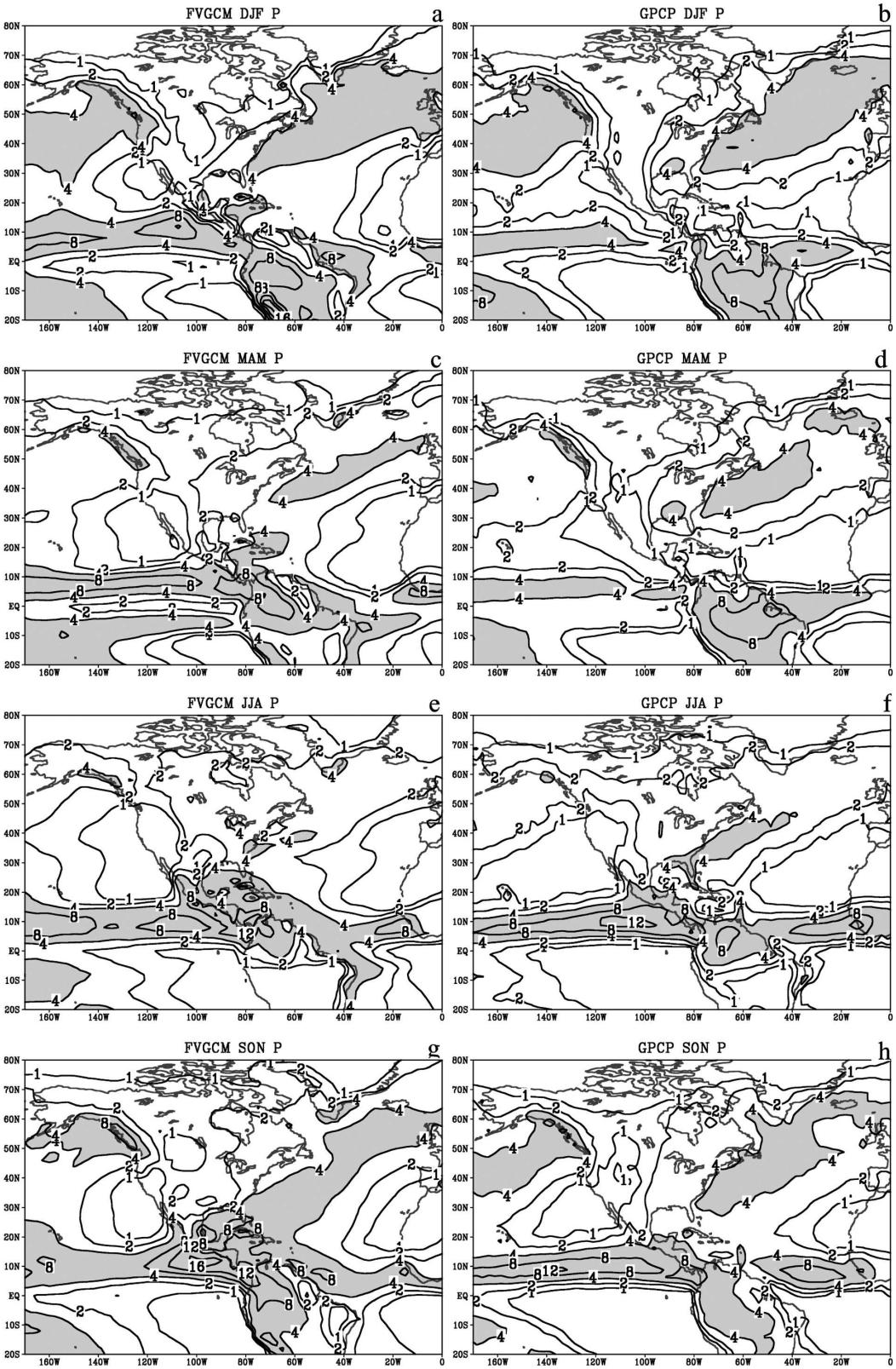

FIG. 2. Seasonal intercomparison of simulated (fvGCM) precipitation with the merged precipitation observations from the GPCP (Adler et al. 2003). The seasons were averaged for December 1979 through November 1997 where the model and observation data coincide. The seasons are (a), (b) DJF; (c), (d) March–May (MAM); (e), (f) JJA; and (g), (h) SON: units are mm day^{-1}; gray shading indicates precipitation rates greater than 4 mm day^{-1}.

product. However, there appears to be an overestimate of precipitation in the northwestern quadrant of the Amazon River basin during SON.

Similarly, the comparison of simulated total precipitable water (TPW) with observations developed by the National Aeronautics and Space Administration (NASA) Water Vapor Project (NVAP) (Simpson et al. 2001) show that the model can reproduce the large-scale patterns (Fig. 3). During SON, the model is wetter than observed over the Amazon basin, while the tropical Atlantic is drier than the NVAP data. The model-simulated TPW over North America during JJA seems reasonable, especially in the regions of MAGS and MRB. There is a dry bias in the simulation over the Rocky Mountains. In general, the model-simulated water cycle data seems comparable to typical AGCMs (Boyle 1998).

In this paper, we will investigate the local influences and atmospheric circulation variations on precipitation recycling in MAGS, MRB, and LBA. The line of investigation emphasizes the 3-month period of maximum precipitation recycling in each basin. Figure 4 shows the basin-averaged major sources of precipitation for each basin. It should be noted that the number of sources for each region is generally a function of the configuration of the source regions (Fig. 1). For example, MAGS has four primary sources of water vapor, likely because the whole North Pacific Ocean's (NPO) evaporation contributes to only one water vapor tracer. Consider that, when the source (in the figure legends) is the same as the destination (Fig. 4a, MAGS; Fig. 4b, MRB; Fig. 4c, LBA), the curve is the basin precipitation recycling. The MAGS seasonal cycle is straightforward, where the Pacific Ocean sources dominate in winter, giving way to continental sources in summer. The 3-month period of maximum precipitation recycling is May–July (MJJ). The size of a region also plays a role in the calculation of a water source; for example, the Asia (ASA) source of water for MAGS reaches a peak in JJA because the continental evaporation is highest in the Asian continent seasonal cycle.

For the MRB, we have discretized the tropical Atlantic Ocean sources further because of many questions regarding the impact of the Gulf of Mexico and Caribbean Sea on the climate of the United States. The MRB seasonal cycle is somewhat more complicated in that the maximum of precipitation recycling occurs during a transition from winter and early spring Pacific Ocean sources to fall tropical Atlantic sources. However, it is a clear annual cycle of precipitation recycling with a maximum in MJJ. Precipitation recycling in LBA (Fig. 4c) is complicated by an extended rainy season. While there is a distinct maximum during the onset season of October–December (OND), a rather high plateau exists from January to February (the wet season). The amount of recycled precipitation is also largest in OND, so we will focus on that time frame for intercomparing between MRB and MAGS.

To evaluate the processes that affect precipitation recycling, beyond the seasonal cycle, we will look at the variability of the water budgets and moisture sources over the 50 years of simulations. Figure 5 shows the time series of precipitation anomalies (from the mean of 1979–97) for the model simulation and GPCP data in the basins of interest and for the seasons of interest (MJJ for MAGS and MRB; OND for LBA). In each of the basins, the GPCP data has a wider range of precipitation anomalies than that of the model simulation. Likewise, Fig. 6 shows the standard deviation, minimum, and maximum of seasonal precipitation in each basin. The general conclusion is that the model simulation variability of precipitation is less than observed, which appears to be a typical result from global model simulations (e.g., Boyle 1998). One exception is the MRB standard deviation, which is near the GPCP value. However, the range of precipitation between maximum and minimum is still smaller in the model simulation.

Another issue is basin-scale trends in the water cycle. The precipitation for each of the basins over the 50 years of simulation does not have trends that are statistically different from zero (Fig. 5, statistics not presented). The model does show some increase in precipitation over the last 25 yr in MAGS and MRB. There is little trend apparent in the GPCP data, either in the basins and seasons considered here or the global mean (Adler et al. 2003). Further evaluation of the other components of the simulated water cycle and their trends will be discussed in section 5.

4. Regional water budgets

The analysis of the model simulation from this point onward focuses on the seasons of maximum precipitation recycling for MAGS (MJJ), MRB (MJJ), and LBA (OND). In this section we evaluate the mean moisture budgets, including the geographical sources of water in the seasonal precipitation, and also the working relationships between the terms of the water budgets, precipitation recycling, and external sources of water. In the following section, we extend this analysis to intercompare local and external forcing on the atmospheric circulation effects on precipitation recycling.

a. MacKenzie River basin

Table 1 shows the basin and time-averaged water balance quantities for the three basins being consid-

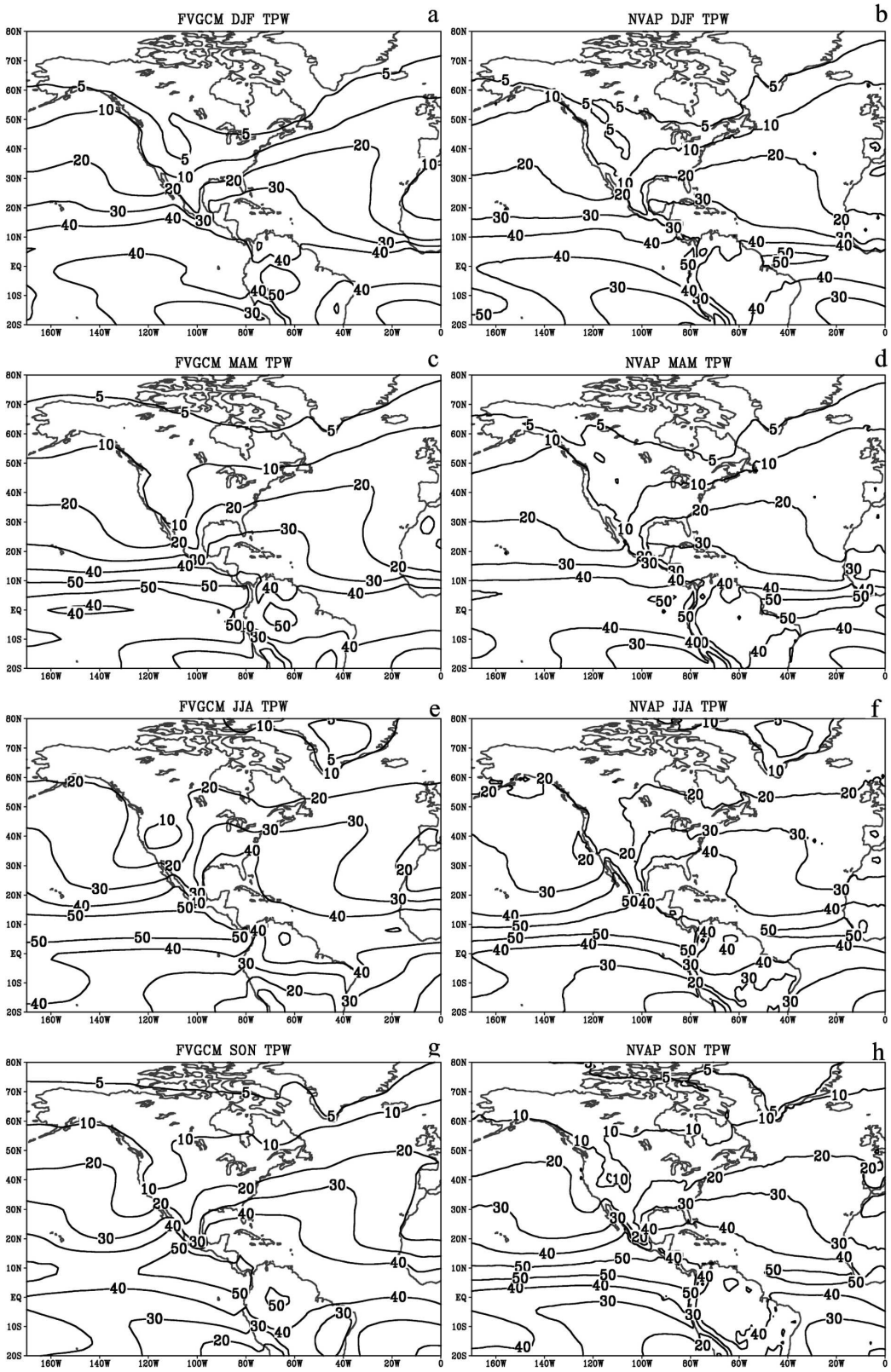

FIG. 3. As in Fig. 2 except for fvGCM simulated TPW and the NVAP observed data (Simpson et al. 2001). The seasons are averaged for December 1988 through November 1999 where the model and observations coincide. The units are mm of water integrated in the atmospheric column.

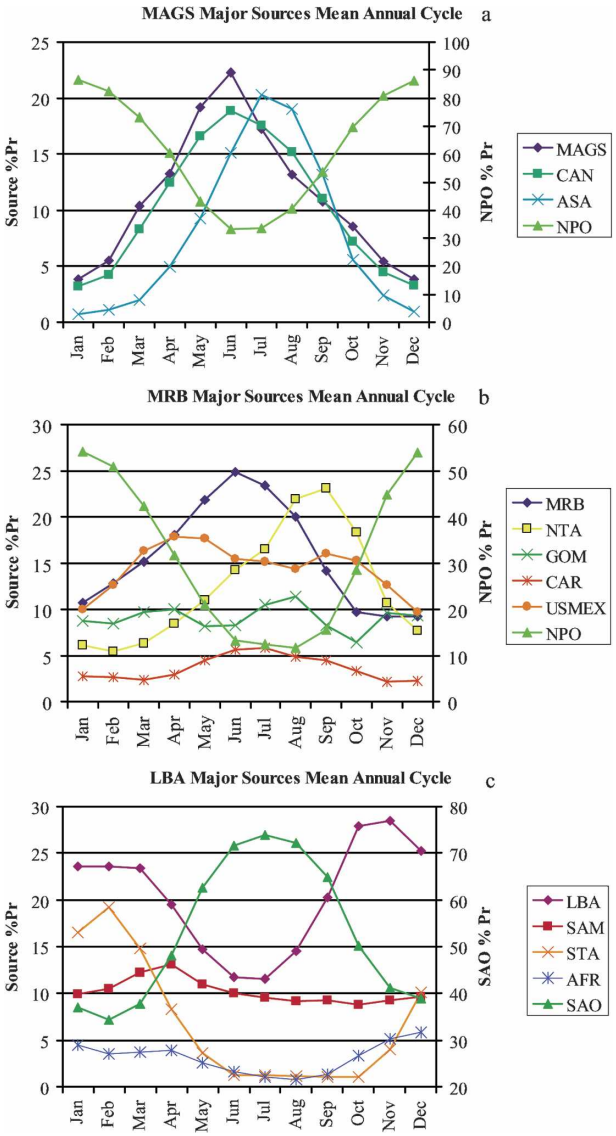

FIG. 4. Mean annual cycle of basin-averaged water sources for MAGS, MRB, and LBA. The colors correspond to the regions in Fig. 1. Note that the major oceanic sources are scaled on the right axis; the label on the right axis corresponds to the specific oceanic source region listed in each legend. The units are percent of total precipitation. Note that the sum of percentages does not equal 100% because only the major contributors are included in these figures.

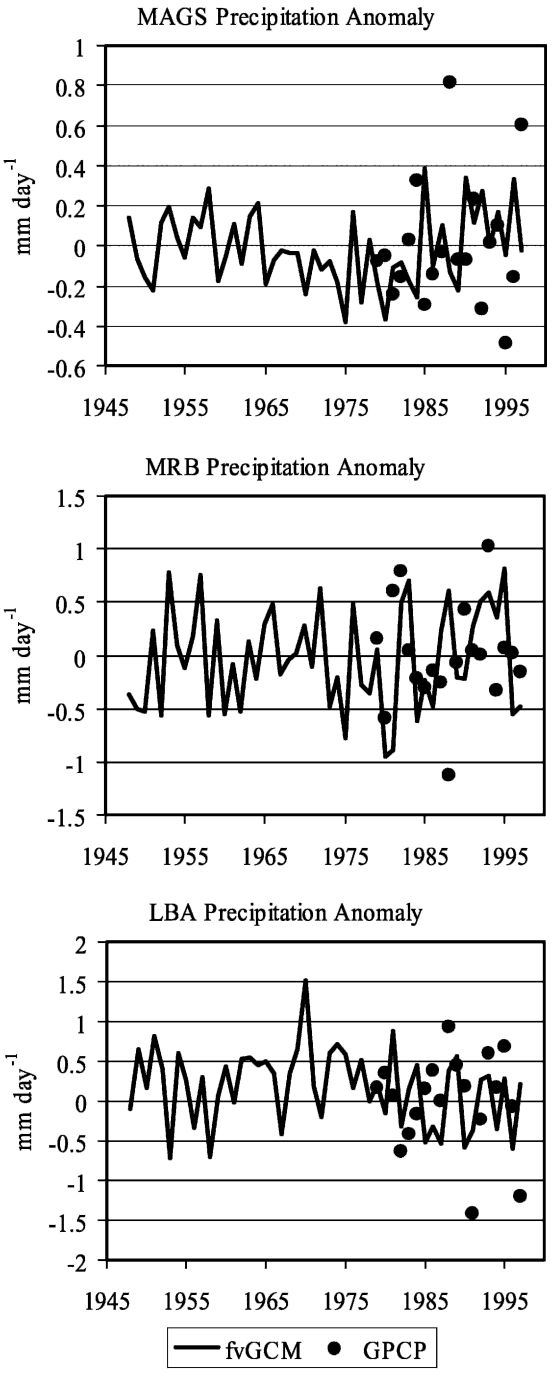

FIG. 5. Time series of precipitation anomalies from the 1979–97 mean for the maximum recycling season in each basin (a) MAGS, (b) MRB, and (c) LBA. The solid line is the model simulation and the dots are GPCP.

ered. In MAGS, evaporation is slightly larger than precipitation, but the primary transport of water vapor is zonal, and the rate of water flux at the zonal boundaries is much more than the average precipitation and evaporation. The recycling ratio in Table 2 for the MAGS basin is almost 20%, meaning that 0.37 mm day^{-1} of the water precipitating in this season has come from evaporation (20% of the 1.9 mm day^{-1} of total precipitation). It is also worthwhile to consider that the percentage of evaporation that stays in the basin is 17% (of the 2.1 mm day^{-1} total evaporation), while the rest is transported out. Using the Eltahir and Bras (1994) bulk diagnostic method for precipitation recycling and re-

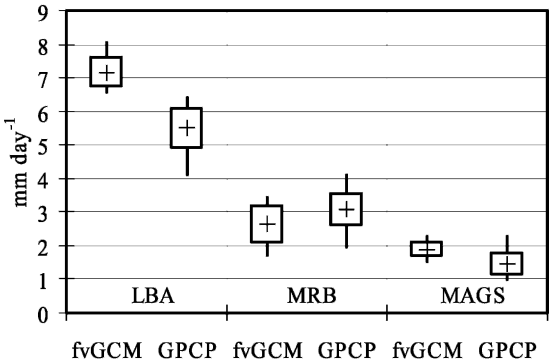

FIG. 6. Mean and variability of the 1979–97 maximum recycling season precipitation time series for the model simulation and the GPCP data in each basin. The + indicates the mean value, the top and bottom of the box shows ±1 std dev from the mean, and the lines indicate the maximum and minimum season precipitation.

analysis input data, Szeto (2002) computed the recycling ratio for MAGS to be 25%.

Even though this is the season when precipitation recycling is maximized in MAGS, the amount of water from the Pacific Ocean almost doubles the local source (36.6% of precipitation comes from the NPO region; Table 2), concurrent with the moisture transport through the western boundary of the basin. However, other land areas including the rest of Canada, and even Asia, also provide significant sources of water. It is important to note that, in the current framework, we cannot more clearly identify source regions beyond the boundaries in Fig. 1.

To better understand the mechanisms by which precipitation recycling occurs, we computed temporal correlations (from the time series of seasonal means for the 50 years of simulation) between the water budget terms and the WVTs (Table 3). Here, we see that the MAGS source for MAGS precipitation (e.g., the precipitation recycling ratio) correlates to precipitation at 0.53, but not as much to evaporation at 0.31. The correlation of recycling ratio to convective precipitation is higher (0.73; not in Table 3). It is interesting to note that the correlations of precipitation with the Pacific Ocean and Asian sources are negative. This indicates that, when precipitation is high, the recycling is high and the external sources are low. The zonal moisture transport also reflects this feature. Given the lack of correspondence between evaporation and precipitation recycling, it appears that the moisture transport variations affect the interannual variations of precipitation recycling in MAGS.

Figures 7a and 7b show a graphical comparison of the major components of the MAGS water budget, namely, total precipitation, evaporation, inflowing moisture, and recycling ratio. This shows that there are exceptions to the conclusions that we might draw from considering only the correlations, by providing distributions to the relationships. However, the magnitude of the recycling ratio still relates more to the amount of water coming in than the variations in surface evaporation, in a general sense. Likewise, higher contributions from the Pacific Ocean can be seen when inflowing moisture is higher, but also in these instances the precipitation is smaller (Fig. 7c). Another issue not included in Tables 1–3 is the impact of snow on the land–atmosphere interactions in MAGS. Snow is still present in this simulation, and is also observed, during May and June (Betts et al. 2003; MacKay et al. 2003). The presence of snow decreases the basin evaporation (Fig. 7d; correlation = −0.71). Higher seasonal averages of snow depth in the basin have lower values of recycling and evaporation. Lower snow depth may have higher evaporation, but there is more scatter in the relation-

TABLE 1. Maximum recycling season time means, area averaged over each basin, MAGS, MRB, and LBA. The variables are P: precipitation; E: evaporation; TPW: total precipitable water; QV: vertically integrated moisture transport at each boundary facing north (N), south (S), east (E), and west (W); ρ: recycling ratio computed from the WVT and Brubaker et al. (1993) bulk (B) methods and the inflowing moisture for the Brubaker et al. (1993) method (Q_{in} is the line-integrated inward transport of water for this method). All units are mm day^{-1} except for TPW (mm) and recycling ratios (percent of total precipitation).

	MAGS	MRB	LBA
P	1.9	2.6	7.3
E	2.1	2.7	3.8
TPW	13.6	23.2	43.8
QV_W	5.0	1.8	−2.7
QV_E	−5.7	−5.9	6.8
QV_S	0.7	5.2	−2.1
QV_N	−0.1	−1.2	1.6
ρ_{WVT}	19.6	23.4	27.2
ρ_B	13.7	14.4	17.5
Q_{in}	6.8	8.1	9.0

TABLE 2. Major precipitation source regions for each basin, MAGS, MRB, and LBA and the percentage of total precipitation during the 3-month season of maximum precipitation recycling (MJJ for MAGS and MRB, and OND for LBA). Region acronyms are identified in Fig. 1.

Rank	MAGS		MRB		LBA	
1	NPO	36.6	MRB	23.4	SAO	43.4
2	MAGS	19.6	US	16.1	LBA	27.2
3	CAN	17.7	NPO	15.5	SAM	9.2
4	ASA	14.9	NTA	13.9	STA	5.1
5	POL	2.9	GOM	8.9	AFR	4.8
6	US+MRB	2.9	CAR	5.3	INO	3.8

TABLE 3. Correlations of water cycle variables during the season of maximum precipitation recycling for (a) MAGS, (b) MRB, and (c) LBA. The variables are defined in Table 1. The percentage of total precipitation from major source regions, as well as precipitation recycling, is also included. In (b), "Trop Atl" indicates the sum of all sources from the tropical Atlantic Ocean (NTA, STA, CAR, and GOM). Values 0.5 or greater are bold; values –0.5 or less are italic.

(a)

MAGS	P	E	$P-E$	TPW	MAGS	NPO	Asia	QV_W	QV_E	QV_S	QV_N	ρ_B
E	0.50	1.00										
$P-E$	**0.81**	−0.10	1.00									
TPW	0.46	0.45	0.22	1.00								
MAGS	**0.53**	0.31	0.40	0.29	1.00							
NPO	*−0.55*	−0.18	*−0.50*	−0.34	*−0.58*	1.00						
Asia	*−0.69*	−0.33	*−0.57*	−0.32	*−0.63*	0.41	1.00					
QV_W	*−0.51*	−0.04	*−0.56*	−0.42	*−0.67*	**0.61**	**0.65**	1.00				
QV_E	**0.59**	0.01	**0.67**	0.49	**0.61**	*−0.52*	*−0.60*	*−0.83*	1.00			
QV_S	0.01	0.34	−0.21	0.07	−0.03	−0.01	0.07	0.04	−0.25	1.00		
QV_N	−0.17	−0.27	−0.01	−0.31	−0.02	−0.04	−0.04	−0.10	−0.26	−0.48	1.00	
ρ_B	**0.63**	0.22	**0.58**	0.44	**0.71**	−0.45	*−0.60*	*−0.76*	**0.81**	−0.05	−0.21	1.00
Q_{in}	*−0.55*	0.04	*−0.66*	−0.34	*−0.61*	0.41	**0.54**	**0.76**	*−0.85*	0.17	0.17	*−0.94*

(b)

MRB	P	E	$P-E$	TPW	MRB	NPO	Trop Atl	QV_W	QV_E	QV_S	QV_N	ρ_B
E	**0.96**	1.00										
$P-E$	**0.83**	**0.64**	1.00									
TPW	**0.57**	**0.55**	0.46	1.00								
MRB	**0.87**	**0.88**	**0.61**	0.41	1.00							
NPO	*−0.54*	*−0.54*	−0.41	−0.43	*−0.58*	1.00						
Trop Atl	−0.36	−0.36	−0.27	0.25	−0.48	−0.03	1.00					
QV_W	0.31	0.31	0.22	−0.13	0.19	0.32	−0.41	1.00				
QV_E	−0.17	−0.12	−0.21	−0.03	0.04	−0.29	−0.01	*−0.69*	1.00			
QV_S	0.40	0.32	0.45	**0.64**	0.05	−0.19	0.40	0.09	*−0.54*	1.00		
QV_N	−0.16	−0.21	−0.03	*−0.54*	−0.04	0.35	−0.34	0.39	*−0.51*	−0.35	1.00	
ρ_B	**0.73**	**0.79**	0.43	0.20	**0.87**	−0.47	*−0.59*	0.17	0.27	−0.26	−0.05	1.00
Q_{in}	0.28	0.24	0.28	0.49	−0.06	−0.06	0.38	0.20	*−0.60*	**0.90**	−0.24	−0.41

(c)

LBA	P	E	$P-E$	TPW	LBA	SAO	STA	QV_W	QV_E	QV_S	QV_N	ρ_B
E	−0.03	1.00										
$P-E$	**0.99**	−0.18	1.00									
TPW	**0.62**	−0.06	**0.62**	1.00								
LBA	0.23	0.27	0.18	−0.04	1.00							
SAO	−0.48	0.08	−0.49	−0.31	*−0.64*	1.00						
STA	0.19	−0.03	0.19	0.33	−0.33	−0.16	1.00					
QV_W	**0.62**	−0.10	**0.62**	0.21	**0.63**	*−0.72*	−0.10	1.00				
QV_E	−0.37	0.08	−0.38	−0.22	*−0.77*	**0.85**	−0.04	*−0.75*	1.00			
QV_S	0.45	−0.08	0.45	0.26	0.42	−0.40	−0.07	0.19	−0.50	1.00		
QV_N	0.42	−0.13	0.44	**0.65**	−0.14	−0.28	**0.64**	−0.06	−0.24	0.24	1.00	
ρ_B	0.05	0.34	0.00	−0.30	**0.87**	−0.48	−0.37	**0.58**	*−0.68*	0.35	−0.41	1.00
Q_{in}	−0.06	0.00	−0.06	0.30	*−0.83*	**0.54**	0.38	*−0.66*	**0.75**	−0.38	0.39	*−0.94*

ship (Fig. 7d). It seems that the partial presence of snow in space and time during this season affects the precipitation recycling, but these interactions are not linear or spatially representative of the whole basin.

b. *Mississippi River basin*

The MRB has some similarities with MAGS regarding the water budget. The maximum recycling season is MJJ in both cases. Also, both have mean evaporation only a small amount greater than the precipitation in this season (Table 1). Being farther south, the MRB TPW is somewhat larger than MAGS, and the convective precipitation is much greater (93% of total precipitation in MRB is convective, compared to 74% in MAGS). The moisture transport from the south boundary is the dominant inflow of atmospheric water. The

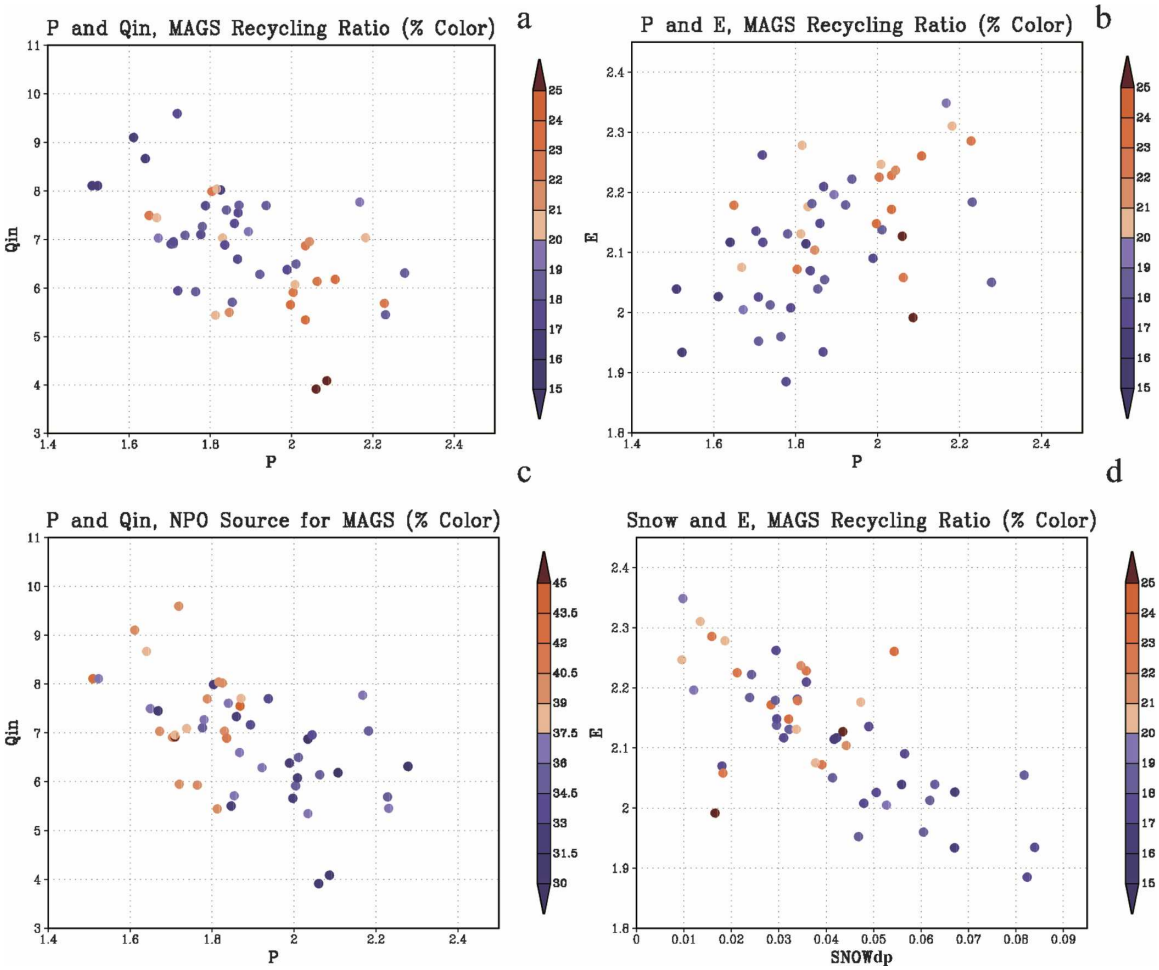

FIG. 7. Scatter diagrams of some of the seasonal and MAGS basin-averaged moisture budget data used to create Table 3a. The figures compare (a) P and Q_{in} with recycling ratio (in color); (b) P and E with recycling ratio (in color); (c) P and Q_{in} with the NPO moisture source (in color); and (d) SNOWdp and E with recycling ratio (in color). Variable names follow the definitions in Tables 1–3 and units are mm day^{-1}, except SNOWdp is the snow depth in meters.

western boundary transport certainly contributes to the basin-scale water cycle, but this varies throughout the season (Fig. 4). The dominant sources of water for the MRB are from the tropical Atlantic Ocean regions (Table 2). While we have disaggregated these sources (including the Gulf of Mexico, Caribbean Sea, and tropical Atlantic Ocean), their combination exceeds the precipitation recycling (also noted by Brubaker et al. 2001). In many meteorological analyses, it is often noted that rain is occurring because of water from the Gulf of Mexico, when wind flows from the south across the southeastern United States. Given the differences in area extent, it is not surprising that the tropical Atlantic Ocean provides more moisture for precipitation than the Gulf of Mexico itself. The dominant oceanic source is then the moist air mass that extends eastward back to Africa. Also, given the area extent of the Pacific Ocean source, it still makes a substantial contribution to the MRB water budget in MJJ (especially in May; Fig. 4b).

The variability of the MRB water budget contrasts MAGS in several key relationships. Most notably, the precipitation and evaporation are highly correlated. Indeed, the precipitation recycling ratio is also highly correlated with both precipitation and evaporation. Bosilovich and Schubert (2001) evaluated the bulk diagnostic precipitation recycling for the central United States in the Goddard Earth Observing System 1 (GEOS 1) reanalysis and found less sensitivity to evaporation. That system used prescribed soil moisture input such that the evaporation could not respond to precipitation. Despite being the largest mean source of water for the MRB, the tropical Atlantic Ocean sources variability does not strongly correlate with total precipitation. To-

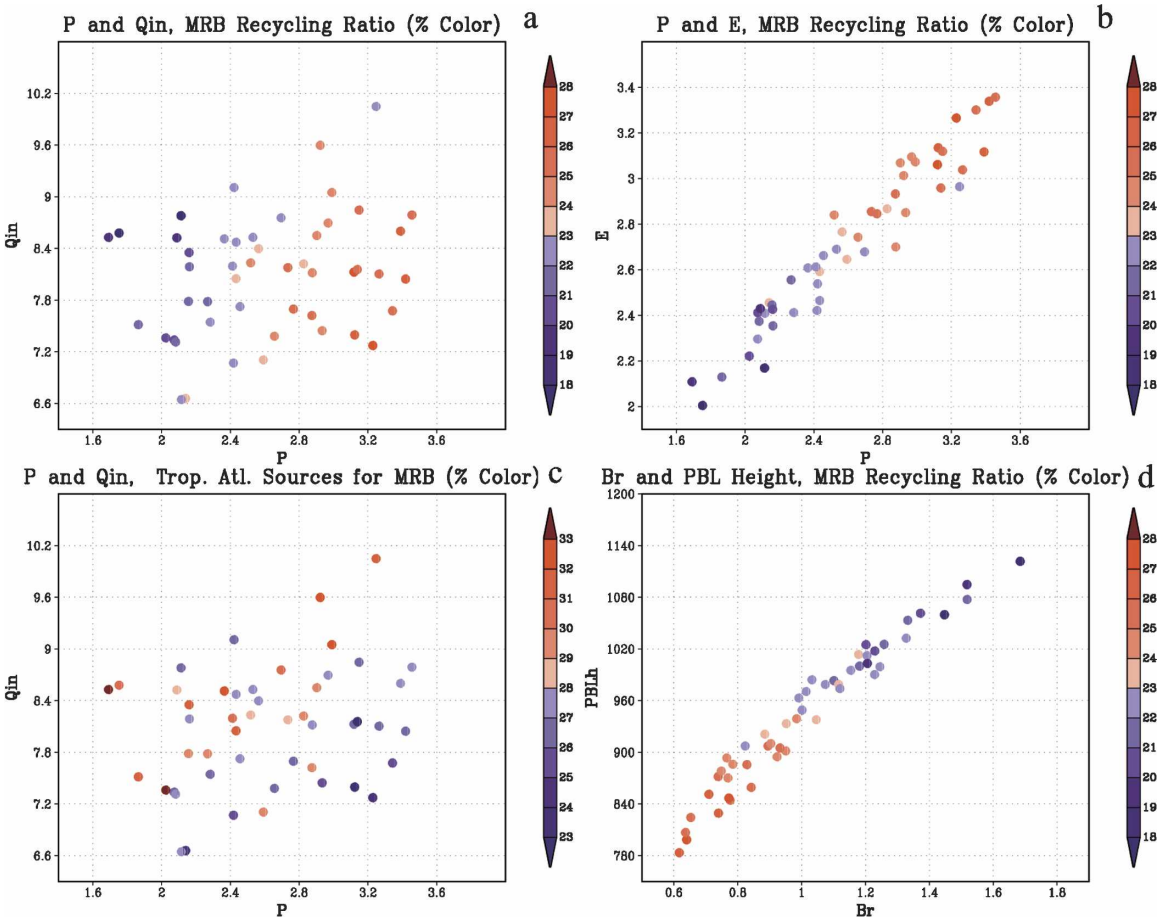

FIG. 8. Scatter diagrams of some of the seasonal and MRB basin-averaged moisture budget data used to create Table 3b. The figures compare (a) P and Q_{in} with recycling ratio (in color); (b) P and E with recycling ratio (in color); (c) P and Q_{in} with the NPO moisture source (in color); and (d) Br and PBLh with recycling ratio (in color). Variable names follow the definitions in Tables 1–3 and units are mm day^{-1}, except Br is the Bowen ratio (sensible heat flux divided by latent heat flux: dimensionless) and PBLh is the depth of the planetary boundary layer in meters.

tal precipitable water does positively correlate with northward transport of water through the south boundary. With the long distance that water has to travel from the tropical Atlantic Ocean to the MRB, the north tropical Atlantic Ocean (NTA) water is mixing throughout the column. Surface evaporation, on the other hand, enters the atmosphere within the PBL and near the cloud base, so it can be entrained into convection, which leads to precipitation recycling (e.g., Bosilovich 2002). Many models show that the central United States is a region where the coupling strength between the land and atmosphere is strong (Koster et al. 2004). Water tracers delineate the local mass of water that contributes to the mass of precipitation, integrating the pathway from evaporation to precipitation, so that precipitation recycling may be another diagnostic of the land–atmosphere coupling.

Figures 8a and 8b show the MRB relationships between precipitation, evaporation, inflowing moisture transport, and recycling ratio. The figure demonstrates the strong linear correlations between P, E, and recycling and low correlation between inflowing moisture with precipitation and moisture transport. The connection between tropical Atlantic Ocean sources with precipitation and moisture inflow is less clearly defined (Fig. 8c). In a general sense, higher contributions from the tropical Atlantic ratios are associated with higher moisture inflow, but with the total precipitation there are substantial variations. This is partly related to somewhat large inflow of moisture that also comes from the Pacific Ocean (Tables 2 and 3). Figure 8d shows the connection between the surface and the planetary boundary layer (PBL) in the MRB. The Bowen ratio is the surface sensible heat divided by the latent heat flux. Sensible heat provides the heating that drives the turbulent mixing of the lowest layers of the atmo-

sphere. When latent heat is high, sensible heat and PBL depth are lower, but the PBL is more moist. Moist boundary layers lead to more recycled precipitation than dry, deep PBLs.

c. Amazon River basin

Precipitation recycling has been considered an important feedback mechanism in the Amazon River basin for some time (Lettau et al. 1979; Eltahir and Bras 1994). The Amazon basin differs substantially from MAGS and MRB, aside from the tropical geographic location. In this experiment, the precipitation and evaporation are much larger than in the other basins. Also, precipitation is much more than the evaporation area averaged in the Amazon basin. The simulated precipitation does exceed the GPCP estimates (Figs. 2 and 6). Basin-averaged precipitation measurements can be approximately 6 mm day^{-1} for this season, and it is a season of transition (Betts et al. 2005; Marengo 2005). The value of evaporation is also low compared to National Centers for Environmental Prediction (NCEP)–NCAR reanalysis, but the model has low interannual variability, which agrees with the reanalysis (Marengo 2004).

The moisture transport into the basin is predominantly from the east, so the South Atlantic Ocean is the primary source of water for precipitation (Table 2). The recycling ratio is 27.2% for this season and, given that the precipitation is so large, the amount of recycled precipitation is 2 mm day^{-1}. The amount of basin evaporation that is recycled is then more than 50%. While it is difficult to intercompare the recycling ratios for different regions (e.g., length scale dependence; Eltahir and Bras 1996), the difference in the amount of evaporation that is recycled between LBA and the MRB and MAGS is likely due to the efficiency of local water to be entrained into convective precipitation. The efficiency may be related to both the tropical environment and the model's parameterization of convective precipitation.

The LBA basin also differs from the MRB and MAGS in that the evaporation has very low interannual variability. This leads to no correlation between evaporation and precipitation (Table 3c). There is also no correlation between the inflowing moisture and precipitation (Table 3c; Figs. 9a and 9b) The soil moisture exceeds field capacity each year so that the interannual variations of evaporation are small. In addition, since evaporation changes little, variations in precipitation recycling are related to changes in moisture transport. When inflowing moisture is strong (weak), the recycling is weak (strong) as in Fig. 9a. Owing to inflowing moisture and weak variability of evaporation, the South Atlantic Ocean and LBA sources are anticorrelated (Table 3; Figs. 9a and 9c). Figure 9b shows the lack of any clear relationship among precipitation, evaporation, and recycling ratio in LBA. However, variations in the Bowen ratio (from surface sensible heating) still relate closely to the thickness of the PBL, as in MRB (Fig. 9d). Similar to MRB, the recycling ratio is generally higher for a shallow PBL and small Bowen ratio. The mean analysis shows that the surface evaporative contribution to precipitation is crucial. However, the correlation between PBL depth and precipitation is −0.82. In the model simulation, when the large-scale atmospheric circulation brings more moisture from the east, the cloudiness is reduced, the PBL thickness is greater (Bowen ratio is larger), and the recycling is lower.

d. Bulk diagnostic precipitation recycling

Bulk diagnostic estimations of precipitation recycling are straightforward derivations and solutions of basin-scale water budgets using monthly mean data (Brubaker et al. 1993; Eltahir and Bras 1994, 1996; Trenberth 1998; Bosilovich and Schubert 2001; Zangvil et al. 2004). For comparison, we implemented the Brubaker et al. (1993) method for each of the basins. This recycling ratio and the inflowing moisture transport (ρ_B and Q_{in}, respectively) are included in Tables 1 and 3. The bulk recycling method tends toward lower values than the WVT recycling ratio calculation. This underestimate is likely a result of the assumptions imposed on the derivation and use of monthly mean data to make the calculation (Bosilovich and Schubert 2002). However, the bulk recycling correlates to the WVT recycling at a very high level for each basin (Table 3). In addition, the bulk recycling calculation appears to reflect similar relationships to precipitation, evaporation, and moisture transport as for the WVT recycling. This suggests that the bulk recycling calculation can represent the interannual variability of recycling as an index. This fortifies the same conclusion by Bosilovich and Schubert (2002) by adding more seasons to the calculation of the correlation and by evaluating more basins.

5. Large-scale interactions

To extend the discussion of the sensitivity of precipitation recycling beyond the local basin-scale water budget, we have evaluated composite years to identify variations in the atmospheric circulation and far-field physical processes. For each basin, we have identified the five highest and five lowest seasonal values of precipitation recycling in the 50-yr time series. Each of these sets of five years is combined together into a com-

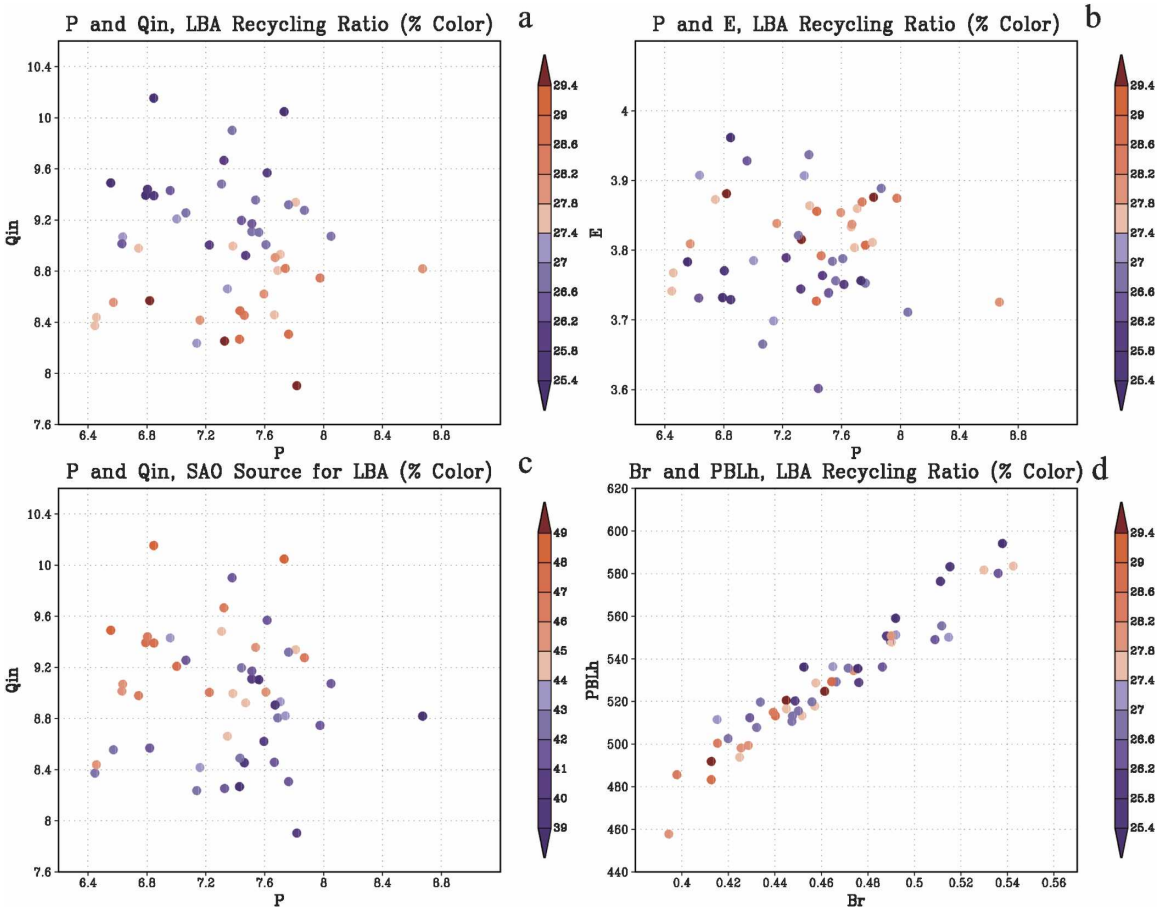

FIG. 9. Scatter diagrams of some of the seasonal and LBA basin-averaged moisture budget data used to create Table 3c. The figures compare (a) P and Q_{in} with recycling ratio (in color); (b) P and E with recycling ratio (in color); (c) P and Q_{in} with the NPO moisture source (in color); and (d) Br and PBLh with recycling ratio (in color). Variable names follow the definitions in Tables 1–3 and units are mm day^{-1}; Br is the Bowen ratio (sensible heat flux divided by latent heat flux; dimensionless) and PBLh is the depth of the planetary boundary layer in meters.

posite. The WVT precipitation recycling for each year of the composites is outside of plus/minus one standard deviation of the basin mean.

a. MacKenzie River basin

Figure 10 shows the mean differences between the MAGS highest and lowest precipitation recycling years. In the 1000–500-hPa thickness field, high values over the region west of MAGS, and low anomalies over the rest of North America, occur when recycling is high. Coincident with the height features is a southward shift of the zonal moisture transport (Fig. 10b). The local positive evaporation anomaly in MAGS is not persistent across the basin. There is a reduction of evaporation in the Pacific Ocean off the west coast of the United States, but this is likely of secondary importance compared to the moisture transport anomaly. West of MAGS through Alaska, the surface temperatures are warm (Fig. 10d), and the soil moisture in the top layers is dry (not shown). In general, the soil moisture anomaly is positive for the interior of MAGS when recycling is high. However, the southerly shift or weakening of the moisture transport reduces the external source of water for precipitation so that, when precipitation occurs, the local sources are relatively higher. Linear trends in the water budget for the MAGS region were also evaluated for the total 50-yr simulation. While there is some increasing precipitation over the last 25 years (Fig. 5a), weak trends in moisture transport and convergence, evaporation, recycling, and external sources of water are not statistically significantly different from zero.

b. Mississippi River basin

In the MRB, high recycling years are characterized by low heights (and 1000–500-hPa thicknesses) over the continental United States (Fig. 11a). The circulation anomaly coincides with a reduction in the northward

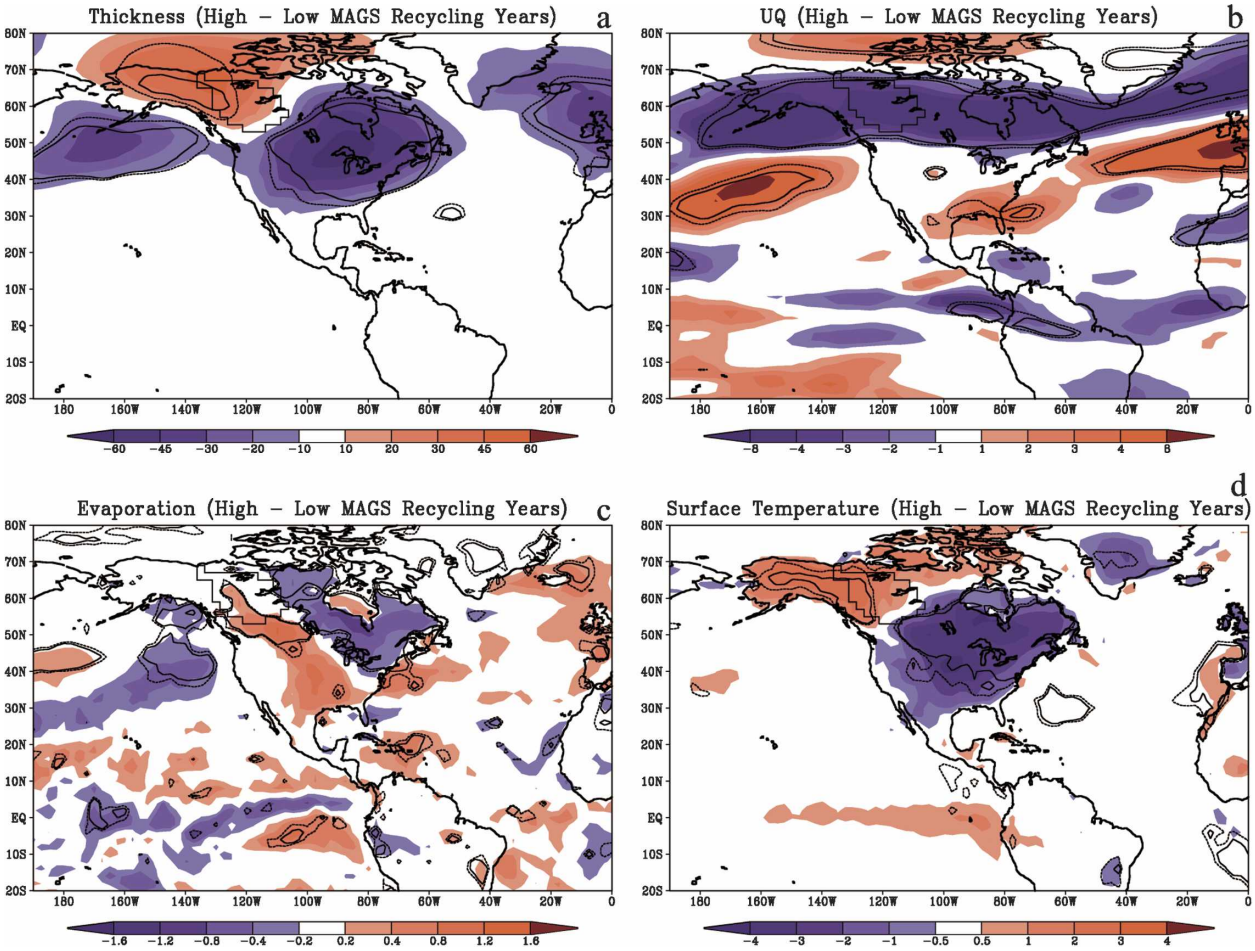

FIG. 10. Mean differences between the five highest and five lowest precipitation recycling years (MJJ) for the MAGS basin of (a) 500–1000-hPa thickness (m), (b) vertically integrated zonal moisture transport (m s^{-1}) (g kg^{-1}), (c) evaporation (mm day^{-1}), and (d) surface temperature (K). The black contours show the statistically significant differences (at the 5% and 10% level). The MAGS basin grid points are outlined.

transport of moisture by the low-level jet (Fig. 11b) and a reduction in the tropical easterly transport of moisture across the Gulf of Mexico (not shown). In the high recycling years, there is ample soil moisture and the evaporation in the basin is generally strong. There is a cold anomaly across the basin, but it extends beyond the basin and the increased evaporation anomaly. The low-level jet provides a large mean source of water vapor for the MRB (Tables 1 and 2). Oglesby et al. (2001) evaluated NCAR CCM3 warm-season precipitation over the MRB, and their differences of wet and dry annual composites are quite similar to Fig. 11. However, their analysis did not extend southward to the tropical oceans.

In high recycling years, SSTs in the equatorial Pacific Ocean are noticeably warm (Fig. 11d). In evaluating extreme events in the U.S. climatology, Trenberth and Guillemot (1996) show that the tropical SSTs had some influence on the MJJ large-scale circulation including the low-level jet, when warm (cold) tropical Pacific SSTs were related to the 1993 flooding precipitation (1988 drought and heat wave). We computed the correlations of the MJJ precipitation and recycling with the Niño-1 + -2 region (0°–10°S, 90°–80°W) SST anomaly in the model. The correlations are positive at 0.38 for precipitation and 0.37 for recycling ratio (0.28 correlation is significantly different from zero at the 5% level). There are occasions when the precipitation recycling is high, but the equatorial Pacific SSTs are cold. Several issues affect the relationships through teleconnections, such as only one realization of the climate in this experiment and the memory of the land surface soil moisture, where deep soil moisture anomalies could persist for some time, affecting the surface evaporation and recycling.

While a weak increasing trend in precipitation seems

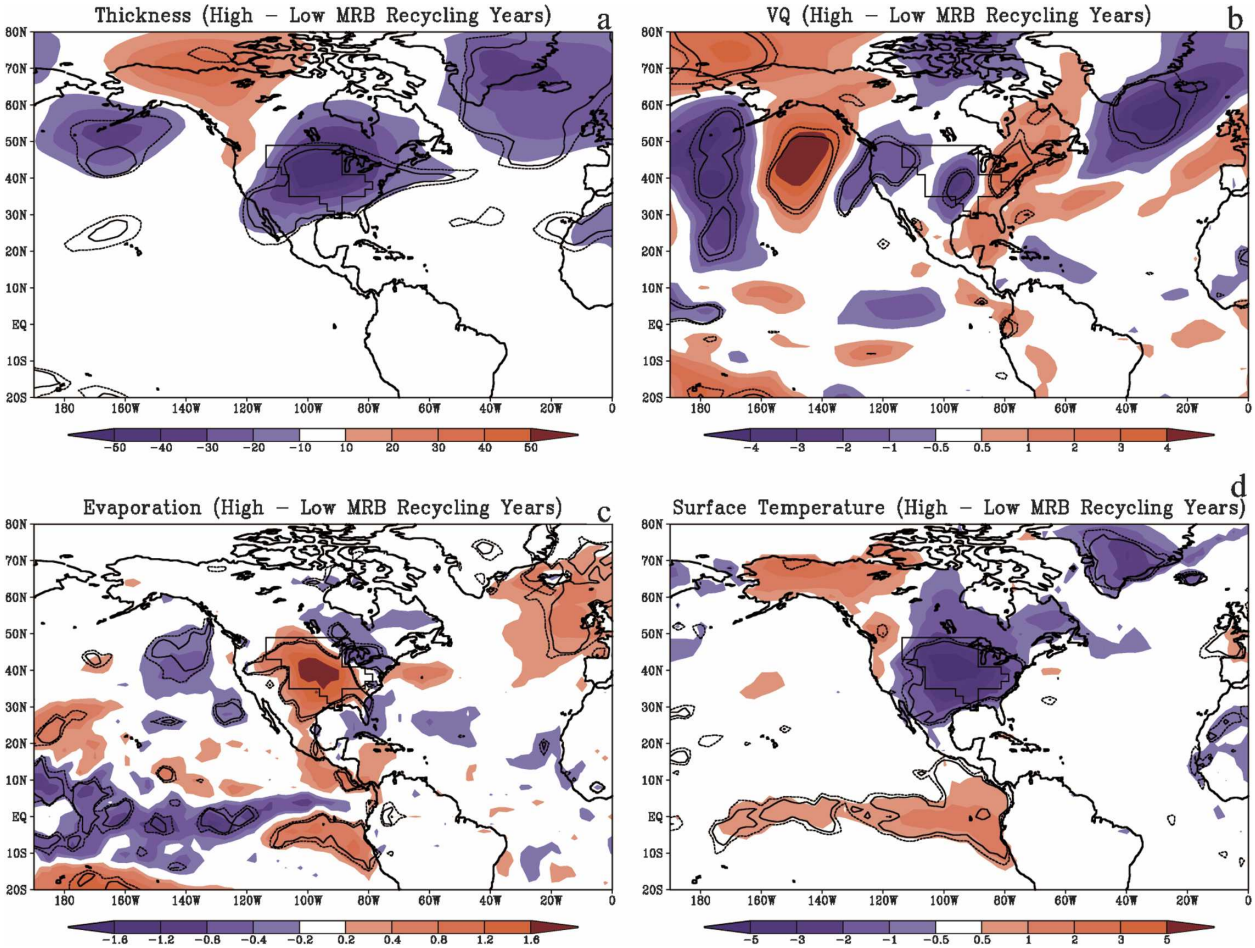

FIG. 11. As in Fig. 10 except for the MRB. (b) The moisture transport is for the meridional component.

to be apparent in the later part of the simulation (Fig. 5b), it is not statistically significantly different from zero. However, the atmospheric circulation and moisture transport did exhibit a trend, apparent in the moisture transport through the region (Fig. 12). The moisture flowing into the basin from the south increases over the 50 years of simulation, but the precipitation, evaporation, and convergence all exhibit little change over the entire period. Likewise, the water tracers do not have a statistically significant trend. Rather, the moisture transport out of the region is increasing with a similar magnitude with no change in the moisture convergence. For this experiment, only mean water cycle diagnostics were saved. Diagnostics relating to the frequency and duration of individual precipitation events were not stored, but could provide more information on the local changes (e.g., Trenberth et al. 2003).

c. *Amazon River basin*

When recycling is high in the LBA basin, the inflow of moisture from the east is reduced (Table 3). The zonal moisture transport anomaly associated with this extends from the southern Atlantic Ocean into the equatorial Pacific Ocean (Fig. 13a) for the extreme (high and low) recycling years. The precipitation anomaly for high LBA recycling is also positive (Fig. 13b), even with less moisture inflow. The precipitation across the Atlantic convergence zone is generally increased for high LBA recycling. Figure 13c is included to contrast the MRB recycling dependency on evaporation with the LBA. The SST anomaly shows cold temperatures in the equatorial Pacific Ocean for high precipitation recycling years (Fig. 13d). These cold temperatures are likely contributing to the weakening of the zonal moisture transport.

In general, SSTs are increasing during these 50 years of simulation, which leads to a general decreasing trend of global precipitation over land (e.g., Bosilovich et al. 2005). The LBA precipitation decreases over the 50 yr (-0.1 mm day^{-1} per decade of annual average precipitation). This is, in part, related to the reduction of recycling in time (Fig. 14). The relationship discussed ear-

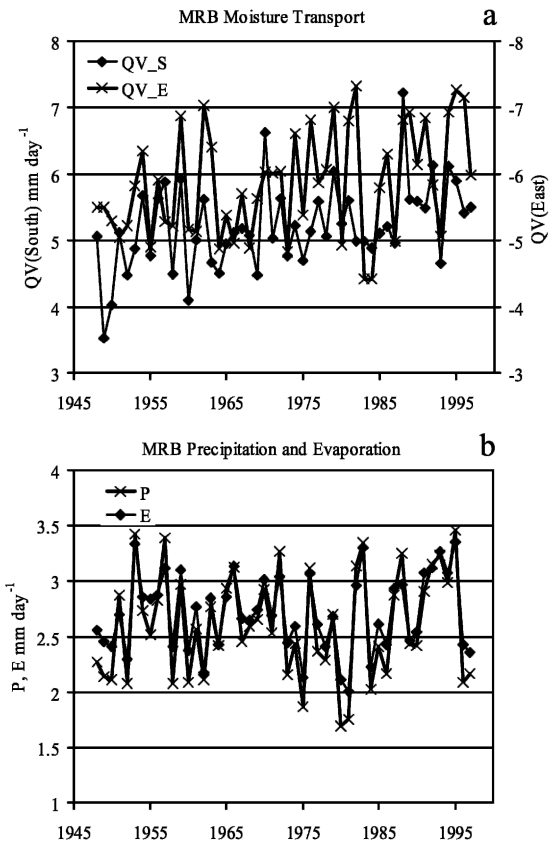

FIG. 12. Time series of MJJ seasonal means for the MRB area average: (a) moisture fluxes into the basin from the south (dots, left axis) and out of the basin (crosses, right axis) and (b) the precipitation (crosses) and evaporation (dots). All units are mm day^{-1}.

lier between recycling and moisture transport is apparent in the time series. The recycling ratio is decreasing by −2.4% and the easterly moisture transport increases by 0.83 mm day^{-1} over the 50 yr. The trends are responding to the SST forcing. Changes in leaf area index and vegetation cover are not included, but might also affect the recycling and feedback.

6. Summary and conclusions

Precipitation recycling is an important process in the water budget and land–atmosphere interactions of a large river basin. However, the mechanisms driving the interactions are not linear and may vary among basins. Here, we evaluate a long AGCM simulation of the water cycle in three river basins with distinct regional differences: MAGS, MRB, and LBA. In addition to the basin-averaged water budget terms, we also include analysis of water sources and precipitation recycling from water vapor tracers and a bulk diagnostic precipitation recycling method. The simulation used the observed SST from the Hadley Centre to prescribe the ocean surface forcing, but no other prescribed time-varying data (e.g., vegetation, carbon dioxide, or aerosols). The model forcing and configuration will be improved in forthcoming Climate of the Twentieth Century experiments (Folland et al. 2002).

Given the definition of precipitation recycling, "the contribution of local evaporation to local precipitation" (Eltahir and Bras 1996), one might assume that the precipitation recycling is a sole function of evaporation. Indeed, without evaporation, there would be no precipitation recycling, and the annual cycle of precipitation recycling tracks evaporation (Bosilovich and Schubert 2001). While most studies include a discussion of the moisture transport (Brubaker et al. 1993; Eltahir and Bras 1996), in some regions the interannual variability of the precipitation recycling is strongly related to the interannual variability of the moisture transport (e.g., MAGS and LBA). In the MRB, there was some concurrent variability of the moisture transport with precipitation recycling, but the sensitivity to evaporation is much larger. This may be expected, as the region has been identified as an area of enhanced land–atmosphere coupling in many models (Koster et al. 2004).

One result that is important for future studies is the strong correlation between recycling ratios calculated from the WVT method and the bulk diagnostic method (Brubaker et al. 1993). The WVT recycling ratios are diagnosed from passive tracers that are predicted forward in time at each model time step. The WVTs experience the diurnal cycle, individual convective events, and synoptic storm systems, while taking up modest computing resources. The bulk diagnostic recycling is computed with monthly mean water budget data after the simulation is completed. The bulk recycling variability in coupled ocean–atmosphere simulations or reanalyses will provide useful information on the local coupling. The weakness of this method is that it cannot account for sources and destinations of water vapor other than the recycling. Other methods can be used to diagnose the water sources in an offline sense, but their complexity and input requirements increase beyond that of the bulk methods.

The current WVT method also has some weaknesses. The source regions are defined at the beginning of the simulation. If, at a later date, a new source region were required, the simulation would have to be performed again. Also, while large-scale sources can be identified (e.g., Pacific Ocean), the regional source geographic locations cannot be identified more specifically. Ideally, if tracer sources could be identified at specific grid

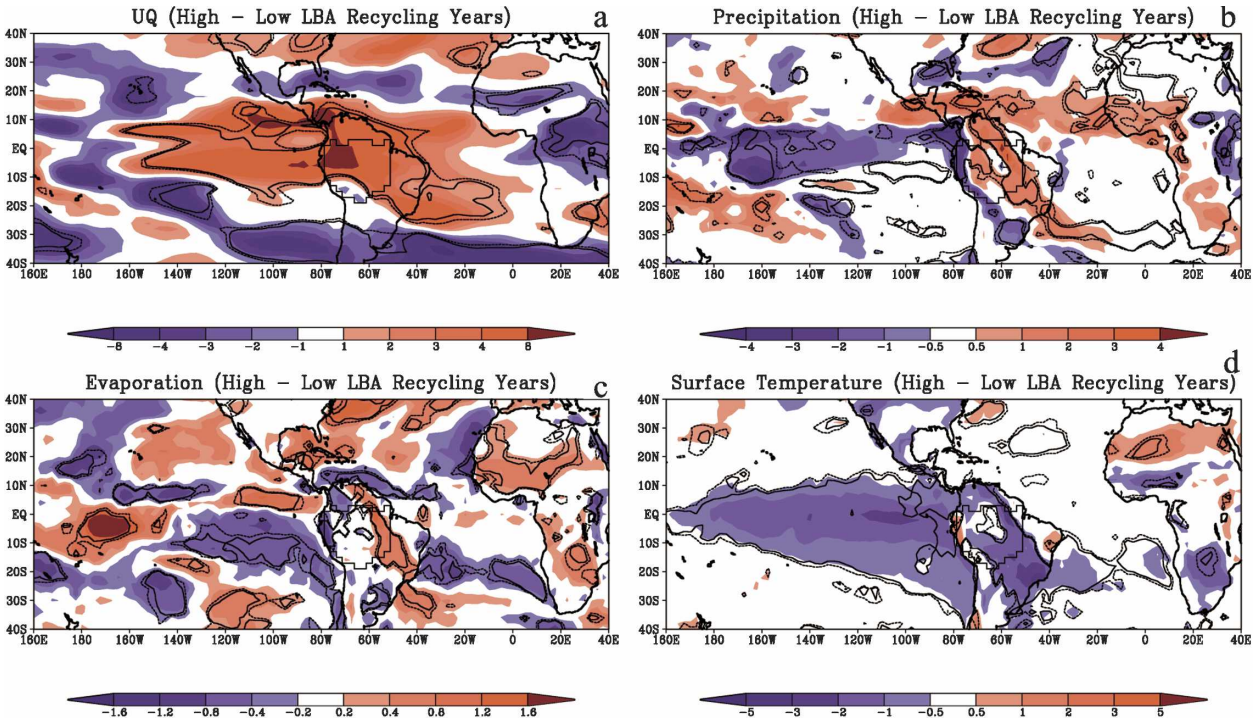

FIG. 13. Mean differences between the five highest and five lowest precipitation recycling years (OND) for the LBA basin of (a) vertically integrated zonal moisture transport [(m s^{-1}) (g kg^{-1})], (b) precipitation (mm day^{-1}), (c) evaporation (mm day^{-1}), and (d) surface temperature (K). The black contours show the statistically significant differences (at the 5% and 10% level). The LBA basin grid points are outlined.

points, the WVT method could be used to identify both forward and backward tracing of water.

Acknowledgments. We appreciate the efforts of Peter Troch, Eric Wood, and the organizing committee of the Catchment Area Hydrological Modeling and Data Assimilation (CAHMDA-II) workshop. The discussions over poster sessions at the meeting were particularly useful in finalizing this manuscript. This work was supported by the NASA Global Water and Energy Cycles program. Thoughtful comments and suggestions from the anonymous reviewers contributed to the final form of this paper.

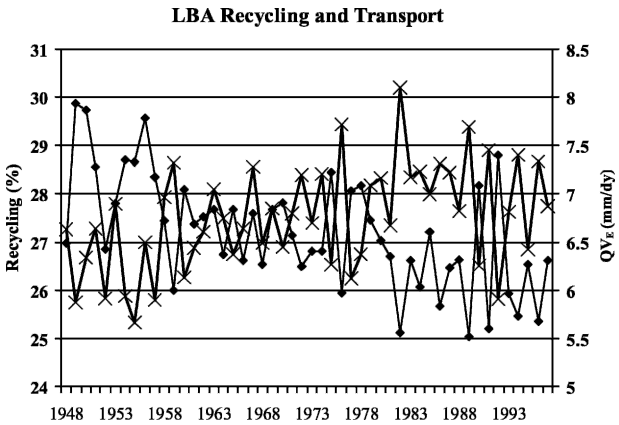

FIG. 14. Time series of OND LBA precipitation recycling ratio (black dots, left axis) and zonal moisture transport from the east (crosses, right axis).

REFERENCES

Adler, R. F., and Coauthors, 2003: The Version-2 Global Precipitation Climatology Project (GPCP) Monthly Precipitation Analysis (1979–present). *J. Hydrometeor.,* **4,** 1147–1167.

Betts, A. K., 2004: Understanding hydrometeorology using global models. *Bull. Amer. Meteor. Soc.,* **85,** 1673–1688.

——, J. H. Ball, and P. Viterbo, 2003: Evaluation of the ERA-40 surface water budget and surface temperature for the Mackenzie River basin. *J. Hydrometeor.,* **4,** 1194–1211.

——, ——, ——, A. Dai, and J. Marengo, 2005: Hydrometeorology of the Amazon in ERA-40. *J. Hydrometeor.,* **6,** 764–774.

Bonan, G. B., K. W. Oleson, M. Vertenstein, S. Levis, X. Zeng, Y. Dai, R. E. Dickinson, and Z.-L. Yang, 2002: The land surface climatology of the Community Land Model coupled to the NCAR Community Climate Model. *J. Climate,* **15,** 3123–3149.

Bosilovich, M. G., 2002: On the vertical distribution of local and remote sources of water for precipitation. *Meteor. Atmos. Phys.,* **80,** 31–41.

——, and S. D. Schubert, 2001: Precipitation recycling in the

GEOS-1 data assimilation system over the central United States. *J. Hydrometeor.,* **2,** 26–35.

——, and ——, 2002: Water vapor tracers as diagnostics of the regional hydrologic cycle. *J. Hydrometeor.,* **3,** 149–165.

——, Y. C. Sud, S. D. Schubert, and G. K. Walker, 2003: Numerical simulation of the large-scale North American monsoon water sources. *J. Geophys. Res.,* **108,** 8614, doi:10.1029/2002JD003095.

——, S. D. Schubert, and G. K. Walker, 2005: Global changes of the water cycle intensity. *J. Climate,* **18,** 1591–1608.

Boyle, J. S., 1998: Evaluation of the annual cycle of precipitation over the United States in GCMs: AMIP simulations. *J. Climate,* **11,** 1041–1055.

Brubaker, K., D. Entekhabi, and P. Eagleson, 1993: Estimation of precipitation recycling. *J. Climate,* **6,** 1077–1089.

——, P. A. Dirmeyer, A. Sudradjat, B. S. Levy, and F. Bernal, 2001: A 36-year climatological description of the evaporative sources of warm-season precipitation in the Mississippi River basin. *J. Hydrometeor.,* **2,** 537–557.

Collins, W. D., and Coauthors, 2004: Description of the NCAR Community Atmosphere Model (CAM2). NCAR Tech. Note NCAR/TN-464+STR, 190 pp.

Dai, Y., and Coauthors, 2003: The Common Land Model. *Bull. Amer. Meteor. Soc.,* **84,** 1013–1023.

Dirmeyer, P. A., and K. L. Brubaker, 1999: Contrasting evaporative moisture sources during the drought of 1988 and the flood of 1993. *J. Geophys. Res.,* **104,** 19 383–19 398.

Eltahir, E. A. B., and R. L. Bras, 1994: Precipitation recycling in the Amazon basin. *Quart. J. Roy. Meteor. Soc.,* **120,** 861–880.

——, and ——, 1996: Precipitation recycling. *Rev. Geophys.,* **34,** 367–378.

Folland, C., J. Shukla, J. Kinter, and M. Rodwell, 2002: The climate of the twentieth century project. *CLIVAR Exchanges,* Vol. 7, No. 2, International CLIVAR Project Office, Southampton, United Kingdom, 37–39.

Hack, J. J., 1994: Parameterization of moist convection in the National Center for Atmospheric Research Community Climate Model (CCM2). *J. Geophys. Res.,* **99,** 5541–5568.

Kiehl, J. T., J. J. Hack, G. B. Bonan, B. A. Boville, D. L. Williamson, and P. J. Rasch, 1998: The National Center for Atmospheric Research Community Climate Model (CCM3). *J. Climate,* **11,** 1131–1149.

Koster, R. D., and Coauthors, 2004: Regions of strong coupling between soil moisture and precipitation. *Science,* **305,** 1138–1140.

Lettau, H., K. Lettau, and L. C. B. Molion, 1979: Amazonia's hydrologic cycle and the role of atmospheric recycling in assessing deforestation effects. *Mon. Wea. Rev.,* **107,** 227–238.

Lin, S.-J., 2004: A "vertically Lagrangian" finite-volume dynamical core for global models. *Mon. Wea. Rev.,* **132,** 2293–2307.

——, and R. B. Rood, 1997: An explicit flux-form semi-Lagrangian shallow-water model on the sphere. *Quart. J. Roy. Meteor. Soc.,* **123,** 2477–2498.

MacKay, M. D., F. Segleneiks, D. Verseghy, E. D. Soulis, K. R. Snelgrove, A. Walker, and K. Szeto, 2003: Modeling Mackenzie Basin surface water balance during CAGES with the Canadian Regional Climate Model. *J. Hydrometeor.,* **4,** 748–767.

Marengo, J., 2004: Interdecadal variability and trends of rainfall across the Amazon basin. *Theor. Appl. Climatol.,* **78,** 79–96.

——, 2005: Characteristics and spatio-temporal variability of the Amazon River basin water budget. *Climate Dyn.,* **24,** 11–22.

Oglesby, R. J., S. Marshall, J. O. Roads, and F. R. Robertson, 2001: Diagnosing warm season precipitation over the GCIP region from a GCM and reanalysis. *J. Geophys. Res.,* **106,** 3357–3370.

Oleson, K. W., and Coauthors, 2004: Technical description of the Community Land Model (CLM). NCAR Tech. Note NCAR/TN-461+STR, 173 pp.

Rayner, N. A., E. B. Horton, D. E. Parker, C. K. Folland, and R. B. Hackett, 1996: Version 2.2 of the global sea-ice and sea surface temperature data set, 1903–1994. Climate Research Tech. Note 74, The Met Office, 35 pp.

——, D. E. Parker, E. B. Horton, C. K. Folland, L. V. Alexander, D. P. Rowell, E. C. Kent, and A. Kaplan, 2003: Global analyses of sea surface temperature, sea ice, and night marine air temperature since the late nineteenth century. *J. Geophys. Res.,* **108,** 4407, doi:10.1029/2002JD002670.

Roads, J. O., M. Kanamitsu, and R. Stewart, 2002: CSE water and energy budgets in the NCEP–DOE Reanalysis II. *J. Hydrometeor.,* **3,** 227–248.

Schubert, S. D., M. J. Suarez, P. J. Pegion, R. D. Koster, and J. T. Bacmeister, 2004a: Causes of long-term drought in the U.S. Great Plains. *J. Climate,* **17,** 485–503.

——, ——, ——, ——, and ——, 2004b: On the cause of the 1930s Dust Bowl. *Science,* **303,** 1855–1859.

Simpson, J. J., J. S. Berg, C. J. Koblinsky, G. L. Hufford, and B. Beckley, 2001: The NVAP global water vapor data set: Independent cross comparison and multi year variability. *Remote Sens. Environ.,* **76,** 112–129.

Stohl, A., and P. James, 2004: A Lagrangian analysis of the atmospheric branch of the global water cycle. Part I: Method description, validation, and demonstration for the August 2002 flooding in Central Europe. *J. Hydrometeor.,* **5,** 656–678.

Szeto, K. K., 2002: Moisture recycling over the Mackenzie Basin. *Atmos.–Ocean,* **40,** 181–197.

Trenberth, K. E., 1998: Atmospheric moisture residence times and cycling: Implications for rainfall rates and climate change. *Climatic Change,* **39,** 667–694.

——, and C. J. Guillemot, 1996: Physical processes involved in the 1988 drought and 1993 floods in North America. *J. Climate,* **9,** 1288–1298.

——, A. Dai, R. M. Rasmussen, and D. B. Parsons, 2003: The changing character of precipitation. *Bull. Amer. Meteor. Soc.,* **84,** 1205–1217.

Yoshimura, K., T. Oki, N. Ohte, and S. Kanae, 2004: Colored moisture analysis estimates of variations in 1998 Asian monsoon water sources. *J. Meteor. Soc. Japan,* **82,** 1315–1329.

Zangvil, A., D. H. Portis, and P. J. Lamb, 2004: Investigation of the large-scale atmospheric moisture field over the Midwestern United States in relation to summer precipitation. Part II: Recycling of local evapotranspiration and association with soil moisture and crop yields. *J. Climate,* **17,** 3283–3301.

Zeng, X., M. Shaikh, Y. Dai, R. E. Dickinson, and R. Myneni, 2002: Coupling of the Common Land Model to the NCAR Community Land Model. *J. Climate,* **15,** 1832–1854.

Zhang, G. J., and N. A. McFarlane, 1995: Sensitivity of climate simulation to the parameterization of cumulus convection in the Canadian Climate Centre general circulation model. *Atmos.–Ocean,* **33,** 407–446.